Journal of Alloys and Compounds 508 (2010) 620–624

Contents lists available at ScienceDirect

Journal of Alloys and Compounds

journal homepage: www.elsevier.com/locate/jallcom

Microwave-hydrothermal synthesis of barium strontium titanate nanoparticles

A.Z. Simões[a,b,*], F. Moura[a,1], T.B. Onofre[a,1], M.A. Ramirez[c], J.A. Varela[c], E. Longo[c]

[a] Universidade Federal de Itajubá- Unifei – Campus Itabira, Rua São Paulo, 377, Bairro: Amazonas, CEP 35900-37, Itabira, MG, Brazil
[b] Universidade Estadual Paulista- Unesp – Faculdade de Engenharia de Guaratinguetá, Av. Dr. Ariberto Pereira da Cunha, 333, Bairro Pedregulho, CEP 12516-410 Guaratinguetá, SP, Brazil
[c] Laboratório Interdisciplinar em Cerâmica (LIEC), Departamento de Físico-Química, Instituto de Química, UNESP, CEP: 14800-900, Araraquara, SP, Brazil

ARTICLE INFO

Article history:
Received 28 May 2010
Received in revised form 25 August 2010
Accepted 27 August 2010
Available online 6 September 2010

Keywords:
Nanoparticle
Chemical synthesis
Microwave
Electron microscopy
Crystal structure

ABSTRACT

Hydrothermal-microwave method (HTMW) was used to synthesize crystalline barium strontium titanate ($Ba_{0.8}Sr_{0.2}TiO_3$) nanoparticles (BST) in the temperature range of 100–130 °C. The crystallization of BST with tetragonal structure was reached at all the synthesis temperatures along with the formation of $BaCO_3$ as a minor impurity at lower syntheses temperatures. Typical FT-IR spectra for tetragonal (BST) nanoparticles presented well defined bands, indicating a substantial short-range order in the system. TG-DTA analyses confirmed the presence of lattice OH– groups, commonly found in materials obtained by HTMW process. FE/SEM revealed that lower syntheses temperatures led to a morphology that consisted of uniform grains while higher syntheses temperature consisted of big grains isolated and embedded in a matrix of small grains. TEM has shown BST nanoparticles with diameters between 40 and 80 nm. These results show that the HTMW synthesis route is rapid, cost effective, and could serve as an alternative to obtain BST nanoparticles.

1. Introduction

Barium titanate has been extensively employed in several industrial applications, including dynamic random access memory (DRAM) capacitor, microwave filters, infrared detectors and dielectric phase shifters, due to their excellent ferroelectric, dielectric, piezoelectric and pyroelectric properties [1–8]. For the ABO_3 perovskite, different A-site and B-site dopants (where A = Ca, Sr, La; B = Nb, Ta, Zr) are used to modify the electrical properties of $BaTiO_3$ based compositions [6–9]. Recently, barium strontium titanate (BST) has attracted much attention because of its strong dielectric nonlinearity under biaselectric field and linearly adjustable Curie temperature with the strontium content over a wide temperature range [9–11]. The desired properties make BST a promising candidate material for tunable microwave dielectric devices [12,13]. To achieve the desired properties, BST needs to be free of intermediate crystalline phases, with a defined stoichiometry and a homogeneous microstructure. Various preparation methods for BST have been investigated. The solid state reaction, starting from $BaCO_3$ or BaO, SrO and TiO_2, is not suitable for preparation of BST ceramics for high performance application because the resulting material shows large particle size and presence of impurities [14]. The main limitation of the solid state reaction is that it requires repeated heat treatments and grinding. The average particle size is normally large and contamination becomes a problem [15].

Wechsler and Kirby [16] prepared BST by conventional mixture containing $BaCO_3$, $SrCO_3$ and TiO_2 fine powders. The resulting microstructure has a wide grain size distribution, multiple phases and an inevitable degree of porosity. Methods such as sol–gel and co-precipitation also have their disadvantages. The sol–gel process utilizes expensive precursors and requires careful control of the atmosphere. The co-precipitation process is limited to cation solutions with similar solubility products. Ries et al. [17] prepared pure barium strontium titanate powder, with Ba/Sr ratio of 80/20 by the polymeric precursor method. The authors have observed that the organic material must be decomposed at low temperatures over a long time to avoid the formation of carbonates.

Among the chemical methods, hydrothermal synthesis is often used due to its simplicity, allowing the control of grain size, morphology and degree of crystallinity by easy changes in the experimental procedure. A variation of this method, microwave assisted hydrothermal synthesis, has the advantage of lower processing temperature and time, and an uniform nucleation of the powders in suspension [18–20]. Studies have been carried out in using different approaches of the hydrothermal technique: Roeder and Slamovich [21] used low temperature hydrothermal reactions while Deshpande et al. [22] used a microwave irradiation to produce BST powder. Both papers discussed processing parameters

* Corresponding author. Tel.: +55 31 3834 6472/6136/12 3123 2765; fax: +55 31 3834 6472/6136.
E-mail address: alezipo@yahoo.com (A.Z. Simões).
[1] Tel.: +55 31 3834 6472/6136; fax: +55 31 3834 6472/6136.

0925-8388/$ – see front matter © 2010 Elsevier B.V. All rights reserved.
doi:10.1016/j.jallcom.2010.08.143

without their impact on dielectric properties of the BST products.

The hydrothermal synthesis route has the most potential in this regard. It is not only found to produce fine powders but is also found to crystallize the tetragonal phase directly from the reaction of hydrated TiO_2 gels and barium chloride in a fairly strong alkali hydroxide solution at a low temperature of 240 °C (pH = 13). In this context, a detailed study on hydrothermal synthesis and characterization of tetragonal $BaTiO_3$ crystallized in the presence of chloride ions at 240 °C has been reported [23]. This study emphasized the role of chloride anion to produce tetragonal phase under hydrothermal conditions. More recently, the formation of a tetragonal phase is also reported in the absence of chloride anions at 220 °C [24]. However, the crystallization kinetics of the tetragonal phase is found to be slow, with crystallization times extending over several days.

Therefore, efforts need to be focused to enhance the crystallization kinetics of hydrothermal process to obtain BST nanoparticles with a high degree of homogeneity and uniform particle size at low temperature. In this study, we have investigated the conditions required for the crystallization of BST under microwave-hydrothermal conditions in the temperature range of 100–130 °C to obtain homogeneous nanoparticles with uniform particle size and low carbonate content.

2. Experimental procedures

The BST nanoparticles were synthesized using ($TiCl_4$ – Sigma–Aldrich 99.95%), Barium acetate ($Ba(CH_3COO)_2$ – Sigma–Aldrich 99%), $SrCl_2{\cdot}6H_2O$ (99%, Mallinckrodt) and NaOH (p.a, Merck). The molar ratio of Ba/Sr was kept at 80/20. Starting materials of $Ba(CH_3COO)_2$ and $SrCl_2{\cdot}6H_2O$ were mixed in distilled water containing 1 M NaOH at 80 °C. The distilled water was boiled for at least 15 min to remove dissolved CO_2 in order to reduce the formation of Ba carbonate. $TiCl_4$ was slowly added to deionized water at 0 °C under stirring until it turned into a homogeneous solution. The solutions were mixed and filtered to remove precipitates from the solution. The solution was transferred into a sealed autoclave and placed in a domestic microwave (2.45 GHz, 800 W). The system was heat treated at 100, 110 and 130 °C for 1 h (heating rate: 10 °C min^{-1}; final pressure 1.2 atm). After that, the pressure vessel was cooled down to room temperature. The resulting powder was washed in distilled water corrected to pH∼12 by 1 M NaOH, filtered and dried in an oven. BST powders were washed with deionized water and dried at 80 °C. The obtained powders were characterized by X-ray powder diffraction (XRD) (Rigaku-DMax/2500PC, Japan) with Cu-Kα radiation (λ = 1.5406 Å) in the 2θ range from 20° to 70° with 0.02° min^{-1}. TG-DTA analyses were carried out with a Netzsch-409 STA apparatus with a heating rate of 20 °C min^{-1} under flowing air. The FT-IR spectra were recorded with a Bruker Equinox-55 instrument. Raman spectra were collected using a Bruker RFS-100/S Raman spectrometer with Fourier transform. A 1064 nm YAG laser was used as the excitation source, and its power was kept at 150 mW. Microstructural characterization was performed by field emission scanning electron microscopy (Supra 35-VP, Carl Zeiss, Germany) and transmission electron microscopy (TEM, Jeol 3010 URP).

3. Results and discussion

Fig. 1 shows typical X-ray diffraction patterns for the nanoparticles obtained at 100, 110 and 130 °C for 1 h. The nanoparticles were perovskite BST, but some intermediate carbonate phase was observed. It can be seen that as the temperature increases, the amount of carbonate decreases. The presence of $BaCO_3$ can be ascribed either to incomplete reaction or due to the presence of carbonate in Ba alkali source. The BST sample crystallized at 130 °C is carbonate free indicating that high temperature hydrothermal technique was successfully used to produce a pure crystalline nanoparticle. All peaks were indexed as a typical perovskite phase (JCPDS card no. 05-0626) with the P4mm space group in a tetragonal structure. An eventual tetragonal peak splitting of the reflections cannot be resolved due to overlapping on the (0 0 2) and (2 0 0) planes. A small amount of orthorhombic Witherite structure, with Pmcn space group, was identified as $BaCO_3$. The obtained results reveal that the chloride ions have an evident effect to

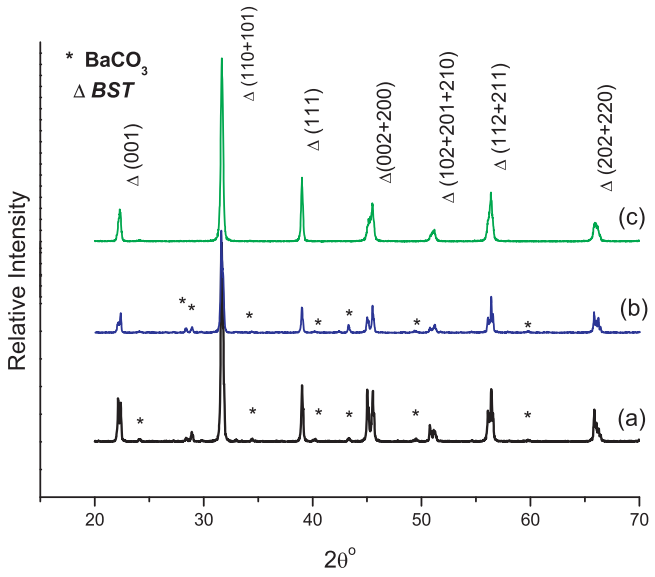

Fig. 1. X-ray diffraction pattern of BST nanoparticles synthesized at (a) 100 °C, (b) 110 °C and (c) 130 °C for 1 h in the HTMW method.

enhance the formation of tetragonal BST under hydrothermal conditions as that reported by Ma et al. [25]. Similar behavior occurred for $Ba_{0.6}Sr_{0.4}TiO_3$ (BST) nanopowders prepared by a modified citrate method with ammonium nitrate as a combustion promoter. In this case, peaks of barium carbonate become weaker when the temperature increased. As the temperature increases to 650 °C, peaks of barium carbonate disappear and a pure BST phase was obtained [26].

Having in mind that BST powder obtained at 130 °C for 1 h is free of carbonates we have performed TG–DTA analyses (Fig. 2). The existence of three stages corresponding to the weight and energy change can be observed. The first region (25–200 °C) corresponds to the loss of physisorbed water; the second between 200 and 350 °C corresponds to the loss of surface hydroxyl groups, and finally, the weight loss above 500 °C is due to CO_2 released from the decomposition of carbonate species. DTA curve shows a strong exothermic peak around 270–350 °C, correlated to a weight loss, that must be considered as the crystallization of the residual amorphous phase.

The FT-IR spectrum of the BST powder obtained at 130 °C for 1 h is plotted in Fig. 3. The absence of carbonate band suggests that the crystallized nanoparticle can further be eliminated at higher temperature, as in agreement with XRD data. The very small absorption band at 1428 cm^{-1} can be interpreted as C=O vibration due to extremely small unavoidable traces of carbonate from environment. Strong intense bands located below 700 cm^{-1} were observed and can be ascribed to δ(M–O) mode. The bands at 3430 and 1644 cm^{-1} correspond to the ν(O–H) mode of (H-bonded) water molecules and δ(OH), respectively. Residual water and hydroxy group are usually detected in the as grown samples and further heat treatment is necessary for their elimination. It is well known that the hydroxylation of metal ions and the deprotonation can be accelerated by raising the solution temperature or pressure [27]. The crystallized nanoparticle was found to have OH^- ions due the alkali used under the present reaction conditions. Furthermore, the hydroxyl content was found to decrease with the increasing of synthesis temperature. This could be due the vigorous action of microwaves to remove such groups at elevated temperature during the hydrothermal process. In hydrothermal-microwave processing the high frequency electromagnetic radiation interacts with the permanent dipole of the liquid (H_2O), which initiates rapid heating from the resultant molecular rotation. Likewise, permanent or induced dipoles in the dispersed phase cause rapid heating of the

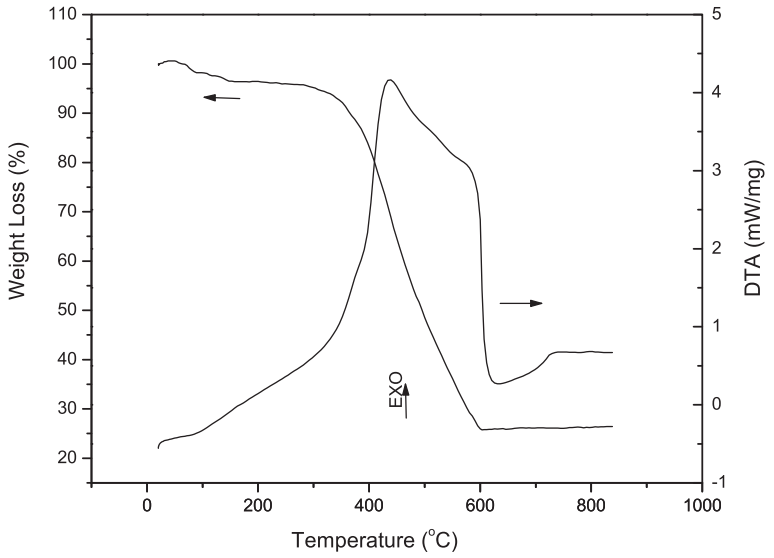

Fig. 2. TG/DTA curves of BST nanoparticle synthesized at 130 °C for 1 h in the HTMW method.

particles. These result in a reaction temperature in excess of the surrounding liquid-localized superheating [28].

The FE/SEM analysis showed that by changing the synthesis parameters, grains with different dimensions could be synthesized. Typical scanning electron micrographs obtained for BST nanoparticles are shown in Fig. 4. The scanning electron micrographs revealed a spherical morphology for all the synthesized nanoparticles. Lower syntheses temperatures led to a uniform morphology that consisted of small grains. On the other hand, the samples thermally treated at higher syntheses temperature consisted of big grains isolated and embedded in a matrix of small grains. The agglomeration process was attributed to Van der Waals forces. To reduce the surface energy, the primary particles have a tendency to form nearly spherical agglomerates, in a minimum surface to volume ratio and hence reducing surface free energy [29,28]. This type of grain structure is common in oxide, ferrite and titanate ceramics [30–37]. This is a result of an abnormal/discontinuous grain growth and also called an exaggerated grain growth. In the abnormal growth, some grains grow faster than others with increasing sintering temperature. The abnormal grain growth may results from: (1) the existence of second phase precipitates or impurities, (2) materials with high anisotropy in interfacial energy and (3) materials in high chemical in equilibrium [38]. In hydrothermally derived BST which crystallizes in a tetragonal structure it can be assumed that the abnormal grain growth comes from factor (1) and (3) because the existence of two-phase structure. At intermediate temperatures, a higher degree of agglomeration was noted. This could be due to the favored nucleation process at higher OH^- concentration with no separation of particles because of low reaction temperature. Based on the morphological evidence, the temperature of 130 °C was found to be optimum to obtain BST nanoparticles with submicron particle size.

Fig. 5 supports the nanometric nature of barium strontium titanate particles obtained at 130 °C by the hydrothermal-microwave method which present diameters between 40 and 80 nm. These values are inside the range of distribution sizes corresponding to tetragonal nanoparticles, according to Kolenko et al. [39]. They observed that samples with particle size smaller than 17 nm present only cubic structure, whereas samples with particles grown larger than this value have only tetragonal structure. As can be seen, the spherical BST nanoparticles are uniform. This result implied that the BST nanoparticles synthesized via the

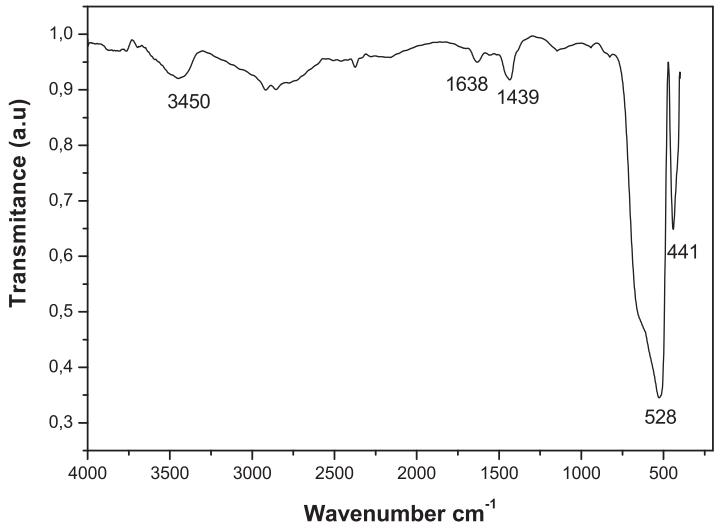

Fig. 3. FT-IR spectra of BST nanoparticle synthesized at 130 °C for 1 h in the HTMW method.

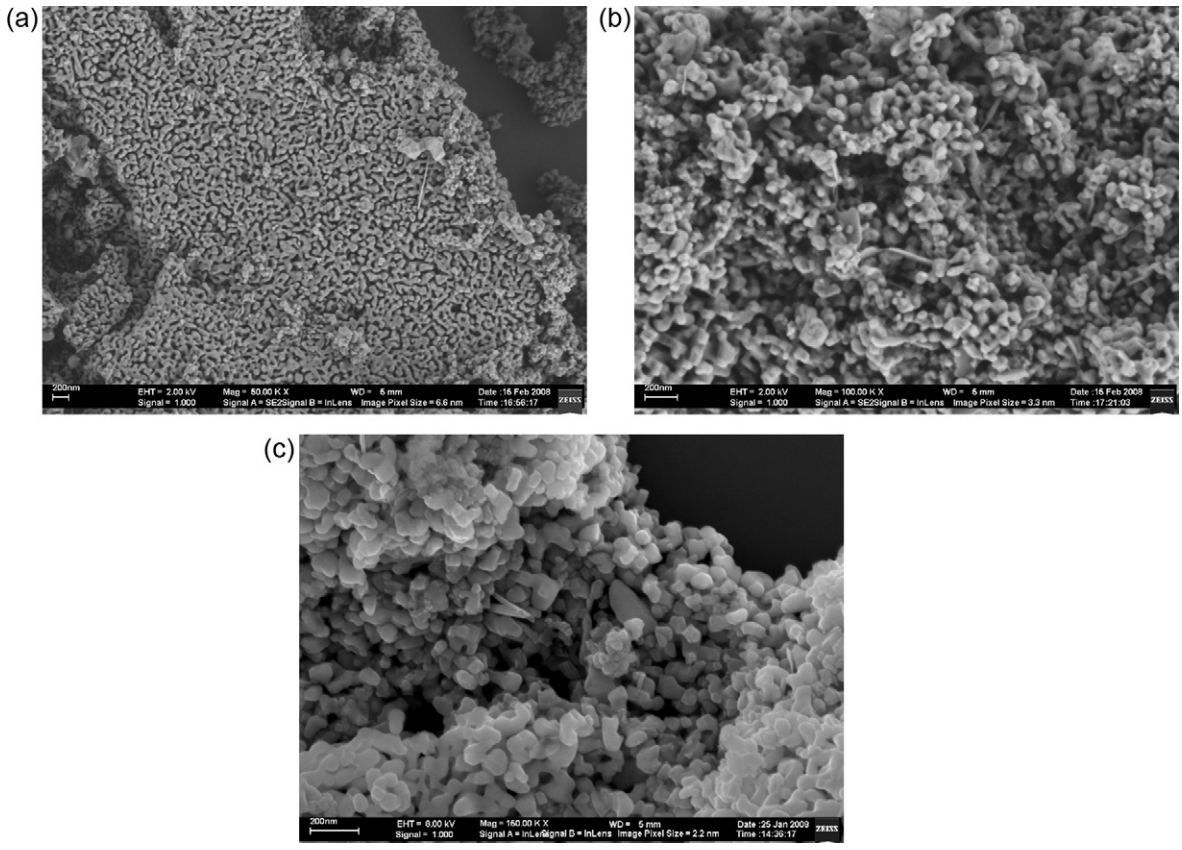

Fig. 4. FE-SEM images of BST nanoparticles synthesized at (a) 100 °C, (b) 110 °C and (c) 130 °C for 1 h in the HTMW method.

rotary–hydrothermal process at 130 °C for 1 h contained very few structural defects. R. Pazik et al. [40] have obtained BST particles doped with Eu from the hydrothermal technique. Most particles are spherical single crystals with an average size of 50 nm. There is no tendency to form clusters and agglomerates as they are mostly separated and not sintered.

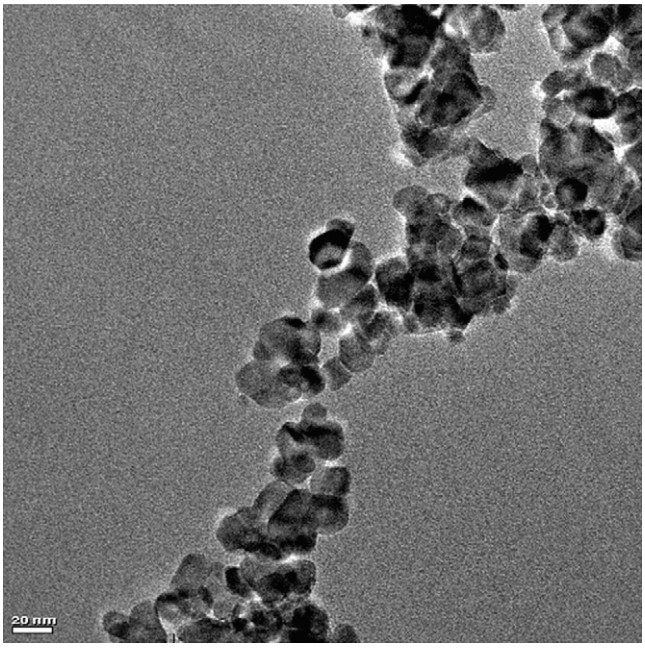

Fig. 5. TEM image of spherical BST nanoparticles synthesized at 130 °C for 1 h in the HTMW method.

4. Conclusions

A simple method to synthesize BST nanospheres by hydrothermal-microwave technique was reported. By varying the processing temperature, nanocrystals having different sizes and distribution could be obtained. XRD analyses confirming the tetragonal structure of the BST nanoparticles, free of carbonates at higher synthesis temperature. The FE/SEM analysis showed that by changing the synthesis parameters, grains with different dimensions could be synthesized. TEM analyses indicate that the BST nanoparticles are uniform indicating very few structural defects. HTMW is interesting not only for the short treatment time and low temperature used, but also for the possibility to control the morphological and structural properties. Therefore, the HTMW method is undeniably a genuine technique for low temperatures and short times in comparison with the above mentioned methodologies.

Acknowledgments

Financial support from the Brazilian agencies FAPESP, CNPq, CAPES is gratefully acknowledged.

References

[1] O.P. Thakur, P. Chandra, A.R. James, J. Alloys Compd. 470 (2009) 548.
[2] H.I. Hsiang, C.S. Hsi, C.C. Huang, S.L. Fu, J. Alloys Compd. 459 (2008) 307.
[3] Z.G. Hu, Y.W. Li, M. Zhu, Z.Q. Zhu, J.H. Chu, Phys. Lett. A 372 (2008) 4521.
[4] S.F. Wang, Y.R. Wang, Y.C. Wu, Y.J. Liu, J. Alloys Compd. 480 (2009) 449.
[5] M. Cernea, E. Andronescu, R. Radu, F. Fochi, C. Galassi, J. Alloys Compd. 490 (2010) 690.
[6] H.Y. Tian, Y. Wang, J. Miao, H.L.W. Chan, C.L. Choy, J. Alloys Compd. 431 (2007) 197.
[7] J.Y. Chen, Y.W. Tseng, C.L. Huang, J. Alloys Compd. 494 (2010) 205.

[8] F. Boujelben, F. Bahri, C. Bouday, A. Maalej, H. Khemakhem, A. Simon, M. Maglione, J. Alloys Compd. 481 (2009) 559.
[9] Q. Xu, X.F. Zhang, Y.H. Huang, W. Chen, H.X. Liu, M. Chen, B.H. Kim, J. Alloys Compd. 488 (2009) 448.
[10] L.N. Su, P. Liu, Y. He, J.P. Zhou, L. Cao, C. Liu, H.W. Zhang, J. Alloys Compd. 494 (2010) 330.
[11] D. Gulwade, P. Gopalan, Solid State Commun. 146 (2008) 340.
[12] P.S. Sahoo, A. Panigrahi, S.K. Patri, R.N.P. Choudhary, J. Alloys Compd. 484 (2009) 832.
[13] X. Chou, J. Zhai, X. Yao, Mater. Chem. Phys. 109 (2008) 125.
[14] Q.X. Jia, H.H. Kung, X.D. Wu, Thin Solids Films 299 (1997) 115.
[15] B.L. Newalkar, S. Komarneni, Mater. Res. Bull. 36 (2001) 2347.
[16] B.A. Wechsler, K.W. Kirby, J. Am. Ceram. Soc. 75 (1992) 981.
[17] A. Ries, A.Z. Simões, M. Cilense, M.A. Zaghete, J.A. Varela, Mater. Charact. 50 (2003) 217.
[18] A. Outzourhit, J. Alloys Compd. 340 (2002) 214.
[19] Q. Roy, H. Li, Mater. Res. Bull. 27 (1992) 1393.
[20] S. Komarneni, Q.H. Li, R. Roy, J. Mater. Res. 11 (1996) 1866.
[21] R.K. Roeder, E.B. Slamovich, J. Am. Ceram. Soc. 82 (1999) 1665.
[22] S.B. Deshpande, Y.B. Khollam, S.V. Bhoraskar, S.K. Date, S.R. Sainkar, H.S. Potdar, Mater. Lett. 59 (2005) 293.
[23] P.K. Dutta, J.R. Gregg, Chem. Mater. 4 (1992) 843.
[24] M. Wu, J. Long, G. Wang, A. Huang, Y. Luo, J. Am. Ceram. Soc. 82 (1999) 3254.
[25] Y. Ma, E. Vileno, S.L. Suib, P.K. Dutta, Chem. Mater. 9 (1997) 3023.
[26] X.H. Zuo, X.Y. Deng, Y. Chen, M. Ruan, W. Li, B. Liu, Y. Qu, B. Xu, Mater. Lett. 64 (2010) 1150.
[27] H. Wang, J.J. Zhu, J.M. Zhu, X.H. Liao, S. Xu, T. Ding, Phys. Chem. 4 (2002) 3794.
[28] G.J. Wilson, A.S. Matijasevich, D.R.G. Mitchell, J.C. Schulz, G.D. Will, Langmuir 22 (2006) 2016.
[29] Y.B. Khollam, A.S. Deshpande, A.J. Patil, H.S. Potdar, S.B. Deshpande, S. Date, Mater. Chem. Phys. 71 (2001) 304.
[30] J. Yoo, The effects of microstructure on $Ba_{1-x}Sr_xTiO_3$ pyroelectric materials for pyroelectric and bolometer infrared sensors, Ph.D. Thesis, University of Auckland, 1999.
[31] A.Z. Simões, M.A. Ramírez, C.S. Riccardi, A. Ries, J.A. Varela, E. Longo, Mater. Chem. Phys. 92 (2005) 373.
[32] A.Z. Simões, M.A. Ramírez, C.S. Riccardi, E. Longo, J.A. Varela, J. Appl. Phys. 98 (2005) 114103–114111.
[33] A.Z. Simões, M.A. Ramírez, C.S. Riccardi, E. Longo, J.A. Varela, Mater. Lett. 60 (2006) 2020.
[34] A.Z. Simões, M.A. Ramírez, C.S. Riccardi, A.H.M. Gonzalez, E. Longo, J.A. Varela, Mater. Chem. Phys. 98 (2006) 203.
[35] A.Z. Simões, M.A. Ramírez, A. Ries, J.A. Varela, E. Longo, R. Ramesh, Appl. Phys. Lett. 88 (2006) 11606–11611.
[36] A.Z. Simões, M.A. Ramírez, B.D. Stojanovic, Z. Marincovic, E. Longo, J.A. Varela, Mater. Sci. Forum 514 (2006) 212.
[37] A.Z. Simões, M.A. Ramírez, A.H.M. Gonzalez, C.S. Riccardi, A. Ries, E. Longo, J.A. Varela, J. Solid State Chem. 179 (2006) 2211.
[38] S.-J.L. Kang, Sintering Densification Grain Growth & Microstructure, Elsevier, Oxford, 2005, p. 265.
[39] Y.V. Kolenko, K.A. Kovnir, I.S. Neira, T. Taniguchi, T. Watanabe, N. Sakamoto, M. Yoshimura, J. Phys. Chem. C 111 (2007) 7306.
[40] R. Pazik, D. Hreniak, W. Strek, A. Speghini, M. Bettinelli, Opt. Mater. 28 (2006) 1284.